Avestia Publishing
Journal of Biomedical Engineering and Biosciences (JBEB)
Volume 12, Year 2025
ISSN: 2564-4998
DOI: 10.11159/jbeb.2025.008

Robotic Laser Microscopy at Tissue Scale: Femtosecond Ablation and Shockwave Probing of Collagen and *Drosophila* Brain

Jiayu Hu*, Sophia Liu*, Xuning Ye*, Rehaan Hassan*, Huiying Huang, Zachary Wang, Veronica Gomez-Godinez, Linda Shi

[1]Institute of Engineering in Medicine, University of California San Diego, La Jolla, CA, 92093
garyhu0420@gmail.com, slliu0129@gmail.com, michaelye2008@gmail.com, rninju812@gmail.com, huh010@ucsd.edu, zaw002@ucsd.edu, vgomez-godinez@ucsd.edu, zshi@ucsd.edu
9500 Gilman Dr. SERF 295, La Jolla, CA, 92093-0435
*High school students participating in IEM OPALS program

Abstract – *Short-pulsed, Robotic-laser microscope systems were shown to be powerful tools for inducing precise and localized damage in live cells to investigate fundamental biomechanics and cellular response pathways. Historically, these systems* ***were*** *applied to live-cell damage in research areas such as DNA repair, cellular biomechanics, chromatin structure during mitosis, and mitotic checkpoint regulation, and neurodegenerative diseases. In this paper, two platforms—femtosecond laser ablation and laser-induced shockwaves (LIS) were applied to analyse tissue-level changes in collagen fibers and were used to probe Drosophila brain tissues. In collagen assays, a measurable ~30% increase in tissue thickness surrounding the ablation zone was demonstrated and was captured by quantitative phase imaging (QPI). In parallel, LIS perturbation of fly brain morphology revealed that total volume, rather than shape, determined resistance to mechanical shock. Collectively, these findings were shown to reinforce the adaptability of laser-induced microscope platforms across biological scales and were found to highlight their applications in tissue engineering, neurodegenerative disease research, and regenerative medicine.*

Keywords**:** Laser-induced Shockwave, Femtosecond Pulsed Laser Ablation, Robotic Laser Microscope Systems, Collagen Tissue, Drosophila Brain Tissue

1. Introduction

Laser-induced microscope systems were established as vital instruments in biomedical engineering, offering non-contact, high-precision tools for manipulating biological materials at cellular and subcellular scales. Mechanical and biochemical properties of cells were probed with exceptional spatial and temporal resolution, and new frontiers in diagnostics, regenerative medicine, and mechanobiology were unlocked. The therapeutic potential of photonic interventions—such as photobiomodulation, laser ablation, and shockwave-based therapies—has been extensively demonstrated in preclinical and translational studies.

Photo-bio-modulation, for example, was shown to modulate microbiota-related dysbiosis [1], to accelerate tendon healing [2], and to promote angiogenesis in ischemic tissues [3]. Low-level laser therapy was reported to enhance osteogenic differentiation and was shown to mineralization in human dental pulp stem cells and modulate macrophage behaviour during bone remodelling [4,5]. In parallel, laser-based technologies have been adapted for oncologic therapies—such as curcumin-gold nanoshells combined with near-infrared irradiation to selectively target ovarian cancer cells [6]—and for molecular-level diagnostics using Raman spectroscopy to assess intracellular photobiomodulation effects [7].

Date Received: 2025-04-08
Date Revised: 2025-09-21
Date Accepted: 2025-10-14
Date Published: 2025-11-25

Building on this evidence, robotic laser microscope systems integrating femtosecond laser ablation and laser-induced shockwave (LIS) modalities were advanced over more than two decades in UCSD Biophotonics Technology Centre. These platforms were used in studies in nuclear DNA damage repair [8], chromatin structure during mitosis [9], and degenerative disease models including Huntington's and Charcot-Marie-Tooth neuropathies [10,11]. LIS was shown to be effective in modelling axonal injury and eliciting neuronal calcium responses in real time, thereby enabling the study of neural mechanotransduction under physiologically relevant conditions [12].

This paper also demonstrated the development of a metasurface-based quantitative phase imaging (QPI) system, inspired by the compound eye structure of birds, which permitted real-time, label-free imaging of nanoscale morphological changes in tissue [13]. This system has been successfully coupled with deep learning-enhanced image reconstruction and has expanded the ability to monitor mechanical perturbations in live biological samples with minimal photodamage.

The application of these robotic laser microscope systems was extended to tissue-level studies for the first time. Specifically, the morphological responses of bovine collagen fibers following femtosecond laser ablation were investigated, and dissected Drosophila melanogaster brain tissues following LIS were examined. By combining QPI and phase contrast imaging, post-ablation collagen remodelling was quantified, and the effect of brain tissue geometry on resistance to mechanical deformation was evaluated. The findings were found to affirm the scalability and precision of our laser platforms and were shown to open new possibilities for tissue engineering, neuroengineering, and laser-assisted diagnostics and therapeutics.

2. Materials and Methods

2.1 Collagen Tissue Ablation and Quantitative Phase Imaging

To investigate the structural response of connective tissue under precise localized laser damage, native type I collagen bundles were taken from bovine Achilles tendon (Sigma-Aldrich C9879; CAS 9007-34-5) and handled at room temperature (20–24 °C). The sample preparation was listed in Table 1.

The robotic laser microscope system III (RoboLase III) was used to cut collagen tissue bundles [8, 10-12]. The system employed a Mai Tai femtosecond laser, beam-routed into a Zeiss inverted microscope Axiovert 200M through a series of highly reflective mirrors. The laser power at the object focal plane was determined by measuring the input energy at the back aperture of the objective multiplied by the transmission factor of the objective at that particular wavelength as shown in [18]. A wavelength of 790 nm, pulse energy of 4 nJ, and average power of 395 mW were set before a 40× objective to target the selected collagen bundle. Ablation was executed precisely along a user-defined line, and images were captured with a QuantEM camera pre- and post-ablation.

The thickness images were acquired using the FOSSMM (Fourier Optics-based Scattering Sensing Metasurface Microscopy) platform [12]. This custom system, developed in collaboration with the Liu labs, integrates metasurface optics inspired by the compound eyes of eagles to produce enhanced quantitative phase imaging (QPI). QPI enables label-free, non-contact visualization of nanoscale refractive index variations in biological samples and was enhanced here by a deep learning-assisted image reconstruction algorithm trained on synthetic and experimental data. Amplitude and phase images were reconstructed to assess changes in fiber thickness and morphology surrounding the ablation zone.

For analysis, image stacks were registered and segmented using FIJI/ImageJ. Tissue thickness at the site of ablation was quantitatively assessed, with pre- and post-treatment averages compared using paired t-tests. QPI resolution limits (~1.12 μm) were noted, and any structures below this threshold were excluded from the final dataset.

2.2 Drosophila Brain Tissue Dissection and Laser-Induced Shockwave (LIS)

To evaluate the biomechanical properties of brain tissue under mechanical stress, Drosophila melanogaster (fruit fly) brains were dissected at 30 days of age [20]. Female brains were harvested in room temperature phosphate buffered saline under a dissection microscope (Olympus). The sample preparation was listed in Table 1.

Brains were imaged within 5 minutes of dissection. Mounting was done by suctioning out the PBS after transferring tissue to an adherent polymer Ibidi 35mm dish(No. 1.5) and slowly adding 200ul of Schneider's insect medium containing Hoechst 33342 (5 μg/mL, Thermo Fisher) for nuclear labelling and

Ethidium Homodimer-1 (EthD-1, 4 μM) to identify compromised cell membranes. Brains damaged during dissection were excluded from shockwave experiments.

Table 1: Sample Preparation

Type	Source	Temp. (°C)	Age	Sex
Collagen tissue	Sigma-Aldrich Type I (C9879)	20–24	NA	NA
D. melanogaster brains	BDSC w¹¹¹⁸ (stock #5905)	20–24	30 days	Female

For LIS stimulation, a Coherent Flare laser system (Spectra-Physics) was employed, operating at a wavelength of 1032 nm, with a 100 Hz repetition rate and a pulse width of 2 ns. Laser power was precisely modulated using a rotating optical polarizer mounted on a stepper-motor-controlled rotation stage (Newport). A mechanical shutter (Vincent Associates), configured with a 10–15 ms duty cycle, was synchronized to permit the passage of 1–2 laser pulses per activation cycle.

Beam expanders were incorporated into the optical path to match the laser beam diameter with the back aperture of the objective lens, ensuring optimal beam focusing. The laser was introduced into the microscope setup via a custom-designed laser entry port (CLEP), and was focused with a 40× PH3 oil-immersion objective (Zeiss Phase III, NA 1.3) mounted on a Zeiss Axiovert 200M inverted microscope. The CLEP's internal filter was set to route pulses to the lower-right quadrant of the imaging field, thereby **maintaining** precise targeting within the specimen plane. The petri dish containing the live brain tissue on stage incubator (Ibidi 37°C and 5% CO_2). Time-lapse imaging was captured using ORCA-Flash4.0 V2 Digital Hamamatsu CMOS camera. Image sequences were acquired before and after the shockwave to assess the brain tissue responses.

3. 3. Results and Discussion

Robotic laser microscopy was applied to tissue-level specimens for the first time. Femtosecond laser ablation and laser-induced shockwaves (LIS) were employed to quantify the biomechanics of collagen fiber networks and to track the morphodynamic responses of dissected *Drosophila* brain tissue under stress. The findings indicated that these platforms provided high spatial resolution, precise actuation, and scalable performance for probing tissue responses to external perturbations.

3.1 Collagen Tissue Response and Structural Remodelling after Laser Ablation

Collagen fiber bundles were visualized on a Zeiss microscope using Phase III contrast. Under identical laser power, the RoboLase laser-microscope system was used to transect thin bundles completely—as shown by the pre-ablation image in Figure 1a and the post-ablation image in Figure 1b. In other cases, partial damage without full transection was observed, with corresponding pre-ablation and post-ablation images shown in Figure 1c and Figure 1d, respectively.

Tissue thickness could not be quantified using conventional brightfield or phase-contrast microscopy. This limitation was addressed by coupling the microscope's right-side port to a QuantEM camera and the metasurface-based quantitative phase imaging (QPI) system FOSSMM [13]. Inspired by avian "eagle-eye" optics, FOSSMM leverages polarization separation and solves the Transport of Intensity Equation (TIE) to generate label-free, high-resolution thickness maps of collagen tissue.

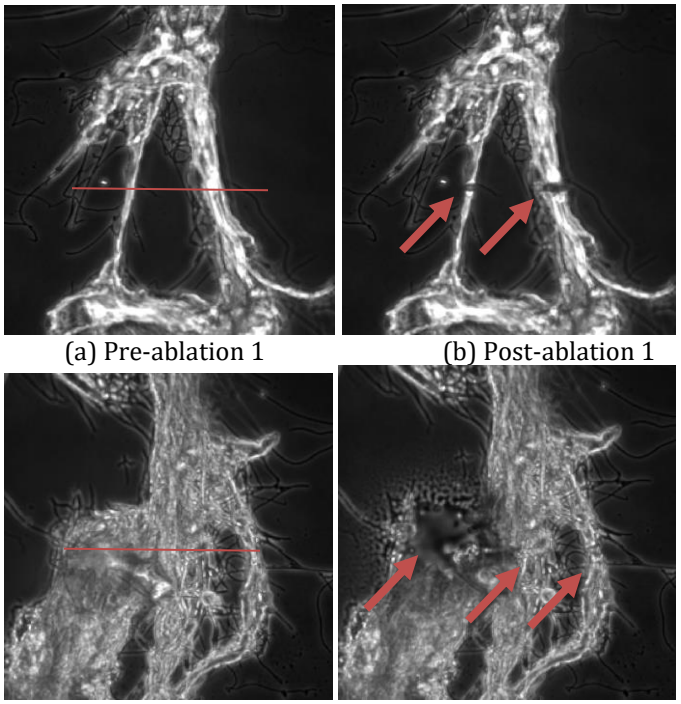

(a) Pre-ablation 1 (b) Post-ablation 1

(c) Pre-ablation 2 (b) Post-ablation 2

Figure 1 Two phase images of collagen fiber under Zeiss Microscope before and after the laser ablation

As illustrated in Figure 2, panels (a) and (b) showed quantitative phase images of collagen fibers imaged via QuantEM camera before and after ablation. Panels (c) and (d) were the quantitative phase images taken of the area indicated by the green dashed frames, and Panels (e) & (f) were the topological views of (c) & (d) respectively, clearly demonstrating the thickening of the tissue post-ablation. This remodelling may reflect laser-induced thermal denaturation, fiber swelling, or partial disruption of collagen crosslinks, triggering localized structural reorganization. This example revealed a significant post-ablation increase in collagen tissue thickness—from an average of 7.78 µm to 10.68 µm, marking a 30% rise.

The use of QPI allowed real-time monitoring without staining or destructive preparation, underscoring the platform's potential for in situ diagnostics of fibrotic remodelling, wound healing, and laser-tissue interactions. While the system achieved excellent spatial accuracy, it was unable to resolve fine structural features under 1.12 µm—such as the narrow ablation line—highlighting the current resolution limit of the system.

Future iterations of this imaging platform may benefit from the integration of higher NA objectives and improved pixel-to-micron mapping to enhance its capacity for nanoscale tissue analysis. Overall, the findings demonstrated that even modest laser doses can induce robust and measurable changes in connective tissue morphology, and the robotic laser microscope system was well-positioned to monitor these changes non-invasively.

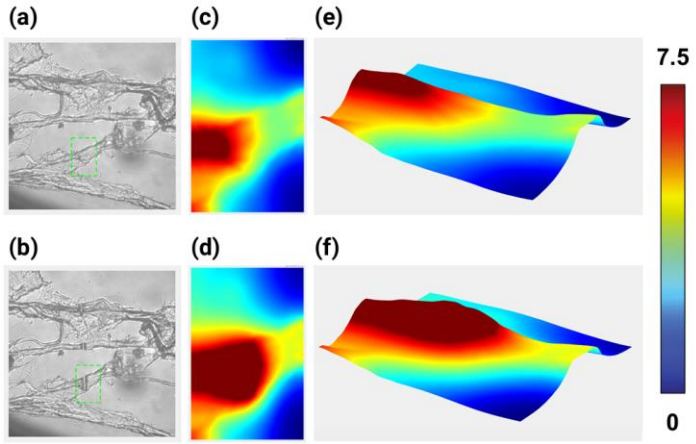

Figure 2. Structural changes in collagen tissue following laser ablation. (a, b) Polarized camera images of collagen fibers before (a) and after (b) femtosecond laser ablation. (c, d) Corresponding quantitative phase images (QPI) generated from the yellow-dashed framed region in (a) and (b), respectively. (e, f) Topographic reconstructions derived from phase data, showing collagen thickening post-ablation

3.2 Drosophila Brain Tissue: Volume-Dependent Shockwave Resistance

In this study, *Drosophila melanogaster* brain tissue was imaged for the first time on a Zeiss fluorescence microscope and was subjected to multiple LIS exposures. Phase contrast images acquired pre-LIS (Figure 3(a)) and post-LIS (Figure 3(b)) demonstrated pronounced morphological alterations consistent with mechanical perturbation. Dead Red fluorescence images obtained pre-LIS (Figure 3(c)) and post-LIS (Figure 3 (d)) indicated an increased prevalence of membrane-compromised cells localized to the shocked region. Together, the phase and viability channels provided complementary evidence of LIS-induced structural and cellular injury in intact brain tissue.

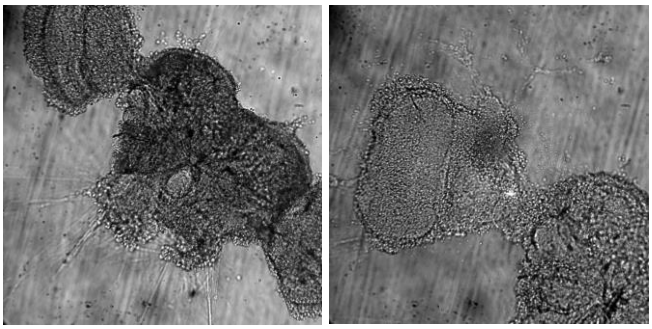

(a) Phase image pre - LIS (b) Phase image post - LIS

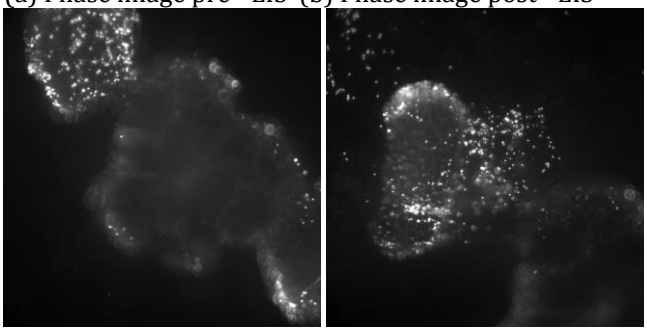

(c) Dead Red pre – LIS (d) Dead Red post – LIS

Figure 3 *Drosophila brain tissue under Zeiss microscope before and after LIS*

To demonstrate precise, volume-based assessment of brain tissue responses, the robotic LIS microscope was used to acquire z-stepped phase and Dead Red fluorescence stacks at 5 µm intervals. Stack registration and voxel calibration were applied to compute tissue volumes and to track displacement after each shockwave exposure (Figure 4; panels a–h).

Two morphologically distinct *Drosophila* brains were analyzed: a wide–flat specimen (base area = 194,132.11 μm²) and a narrow–tall specimen (base area = 116,924.39 μm²) as shown in Figure 4. Despite the contrasting footprints, comparable in-plane displacements and similar EthD-1–positive signals were observed across exposures. Full displacement was reached after a cumulative depth of 15 μm (three LIS pulses) for the wide–flat brain, whereas 25 μm (five pulses) was required for the narrow–tall brain. Volumetric reconstructions yielded near-identical totals—2.91 × 10^6 μm³ and 2.92 × 10^6 μm³, respectively—indicating that total volume, rather than footprint or shape alone, governed resistance to mechanical shock.

Together, the phase and viability channels provided a synchronized readout of structural deformation and membrane compromise, while the z-stack workflow enabled precise, repeatable volume measurement. These results support the use of the LIS microscopy platform for quantitative, volume-resolved characterization of brain tissue mechanics and position it for applications in experimental TBI and tissue-level resilience studies.

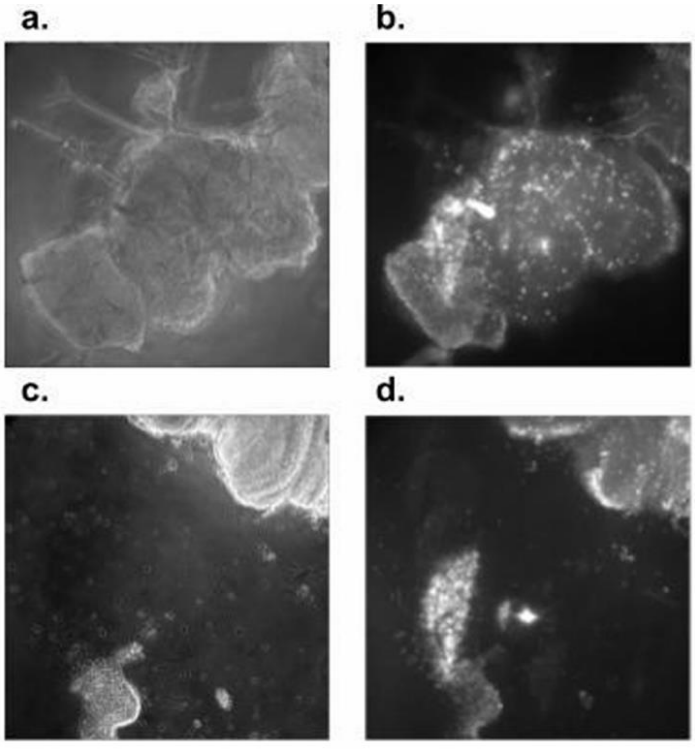

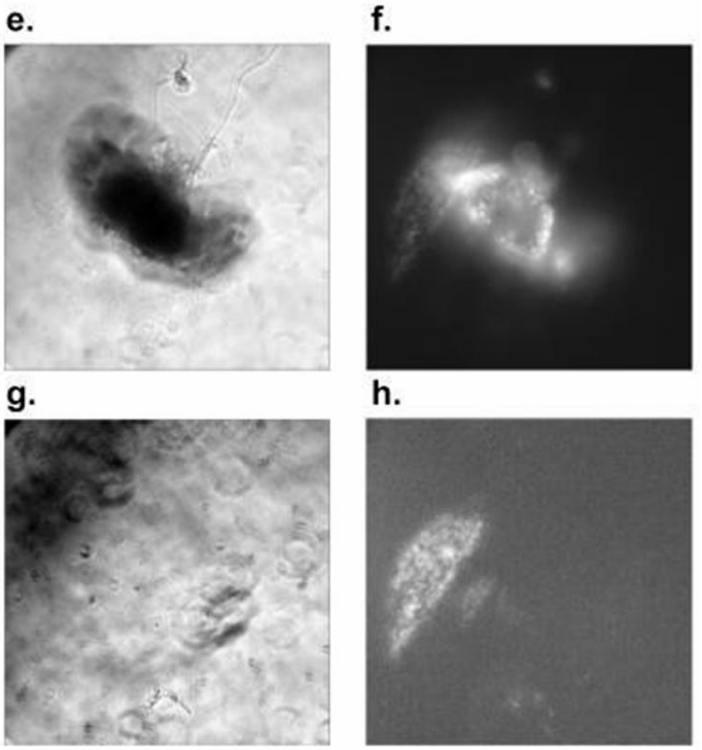

Figure 4. Comparative analysis of two morphologically distinct Drosophila brain tissues subjected to laser-induced shockwaves. (a–b) Wide-flat brain morphology at the initial focal plane captured in phase contrast and EthD-1 (Dead Red) fluorescent channels, respectively. (c–d) The same tissue after full displacement following three LIS exposures at 5 μm intervals (15 μm total), visualized in phase and fluorescence. (e–f) Narrow-tall brain morphology at the initial focal plane in phase contrast and EthD-1 channels. (g–h) Tissue post full displacement after five LIS exposures at 5 μm steps (25 μm total)

3.3 Broader Implications and Technological Validation

Collectively, these results validated the robotic laser microscope systems as reliable tools for biomechanical studies at the tissue scale. The high reproducibility across replicates supported the robustness of the workflow. By integrating deep learning-assisted QPI with precision on the laser ablation system and LIS on the other system extended the scope from the cellular level to tissue-level mechanobiology, damage simulation, and diagnostics.

This versatility opened several research directions. First, the clear structure-function relationships uncovered in collagen and brain tissues suggested extensions patient-derived organoids, engineered scaffolds, and decellularized matrices. Second pairing

laser ablation and LIS systems with outputs with machine-learning classifiers was expected to accelerate discovery of mechanical biomarkers. In addition, controlled perturbations could be used as programmable assays for preclinical drug screening and evaluation of targeted therapies in soft-tissue disease.

4. Conclusion

This study represented a pivotal step in extending the capabilities of the robotic laser microscope systems—originally designed for cellular-level investigations—into tissue-level applications with high spatial precision and functional relevance. By integrating femtosecond laser ablation and laser-induced shockwave (LIS) technologies with advanced imaging modalities such as quantitative phase imaging (QPI) and fluorescence microscopy, feasibility was demonstrated for tracking dynamic structural and biomechanical changes in extracellular matrices (collagen) and complex neuronal tissues (Drosophila brain).

Sensitivity to morphological adaptation was confirmed, including significant post-ablation thickening in collagen fibers, and a volume-dependent determinant of mechanical resilience was revealed in brains exposed to repeated shockwaves. Consistent displacement patterns across distinct brain geometries indicated that total tissue volume can serve as a predictive parameter for integrity under mechanical stress.

A recent Nanophotonics study (Aug 6, 2025) introduced a dual-mode varifocal Moiré metalens that combines TIE-based QPI with polarization-switchable edge-enhanced imaging, reporting ∼1.3 μm minimum spatial resolution and QPI RMSE ≈0.015 rad [19]. This aligns with our current observation that features <∼1.1 μm are difficult to resolve in our setup and motivates a higher-NA confirmatory set and explicit resolution benchmarking.

Present work uses ex vivo brain prep; ablation temperature not tracked; The future work will (i) repeat key runs with higher-NA optics and finer sampling with bead/target resolution controls, (ii) regress displacement vs. measured volume across additional tissue levels.

These findings carry implications for multiple fields, including neuroengineering, regenerative medicine, and tissue biomechanics. The ability to induce and monitor controlled microtrauma in both soft connective tissue and neuronal tissues provided a platform for studying injury response, repair processes and therapeutic mechanisms for testing biomaterials; for evaluating drug candidates; and for informing multiscale computational models of trauma.

Future development includes the integration of artificial intelligence and machine learning for automated damage classification and improved interpretation of phase and fluorescence signals, expansion in vivo for longitudinal studies of injury and healing, and coupling with optogenetic and electrophysiological readouts to enhance real-time mechanobiology. Future investigations will involve shockwaving similar brain areas for better comparisons.

In sum, tissue-level applicability of the robotic laser platforms was validated, and a pathway was established for broader use in next-generation biomedical research that links cellular phenomena to whole-tissue physiology.

Acknowledgements

The authors would like to thank Dr. Lingyan Shi's lab for providing the fruit flies (Drosophila), and Dr. Wei Xiong's lab for providing the collagen samples. This study was based upon work supported by a gift from Beckman Laser Institute Inc. to LS & VGG. Special thanks to the private donors to our UCSD IEM BTC centre: Dr. Shu Chien from UCSD Bioengineering, Dr. Lizhu Chen from CorDx Inc., Dr. Xinhua Zheng, David & Leslie Lee for their generous donations.

References

[1] M. Pourhajibagher, F. Gharibpour, N. Nikparto, R. Bahrami, and A. Bahador, "The effect of photobiomodulation on oral microbiota dysbiosis: A literature review," *Photodiagnosis and Photodynamic Therapy*, vol. 52, p. 104525, Apr. 2025, doi: 10.1016/j.pdpdt.2025.104525.

[2] J. K. Lim, J. H. Kim, G. T. Park, S. H. Woo, M. Cho, and S. W. Kang, "Efficacy of Light-Emitting Diode-Mediated Photobiomodulation in Tendon Healing in a Murine Model," *International Journal of Molecular Sciences*, vol. 26, no. 5, p. 2286, Mar. 2025, doi: 10.3390/ijms26052286.

[3] P. H. Sung, J. N. Yeh, T. C. Yin, H. T. Chai, J. Y. Chiang, C. R. Huang, Y. L. Chen, M. S. Lee, and H. K. Yip, "Extracorporeal shockwave therapy rescued mouse critical limb ischemia via upregulating GPR120 against inflammation and promoting angiogenesis for restoring the blood flow in ischemic zone—experimental study," *International Journal of Surgery*, vol. 111, no. 3, pp. 2414–2429, Mar. 2025, doi: 10.1097/JS9.0000000000002243.

[4] R. Yoshida, K. Kobayashi, K. Onuma, R. Yamamoto, R. Chiba-Ohkuma, T. Karakida, S. Yamakawa, N. Hosoya, Y. Yamazaki, and Y. Yamakoshi, "Enhancement of differentiation and mineralization of human dental pulp stem cells via TGF-β signaling in low-level laser therapy using Er:YAG lasers," *Journal of Oral Biosciences*, vol. 67, no. 1, p. 100617, Mar. 2025, doi: 10.1016/j.job.2025.100617.

[5] K. Mayahara, R. Okuma, T. Sasagawa, M. Motoyoshi, and N. Shimizu, "Effects of low-level laser irradiation on osteoclastogenesis in prostaglandin E2-stimulated macrophages," *Lasers in Medical Science*, vol. 40, no. 1, p. 163, Mar. 2025, doi: 10.1007/s10103-025-04423-w.

[6] S. Rokhgireh, S. Chaichian, A. Mehdizadeh Kashi, B. Haji Ali, K. Tehermanesh, M. Ajdary, S. Nasir, V. Pirhajati Mahabadi, and N. Eslahi, "Curcumin-gold nanoshell mediated near-infrared irradiation on human ovarian cancer cell: in vitro study," *Medical Oncology*, vol. 42, no. 5, p. 145, Apr. 2025, doi: 10.1007/s12032-025-02687-4.

[7] M. Rastogi, A. Chowdhury, S. Chakraborty, K. Sahu, and S. K. Majumder, "Label-free and real-time assessment of 660 nm red light photobiomodulation induced molecular alterations in human adipose-derived mesenchymal stem cells using micro Raman spectroscopy," *Spectrochimica Acta Part A: Molecular and Biomolecular Spectroscopy*, vol. 329, p. 125552, Mar. 2025, doi: 10.1016/j.saa.2024.125552.

[8] M. L. Duquette, Q. Zhu, E. R. Taylor, A. J. Tsay, L. Z. Shi, M. W. Berns, and C. H. McGowan, "CtIP is required to initiate replication-dependent interstrand crosslink repair," *PLoS Genetics*, vol. 8, no. 11, p. e1003050, 2012, doi: 10.1371/journal.pgen.1003050.

[9] S. B. Shah, Y. Li, S. Li, Q. Hu, T. Wu, Y. Shi, T. Nguyen, I. Ive, L. Shi, H. Wang, and X. Wu, "53BP1 deficiency leads to hyperrecombination using break-induced replication (BIR)," *Nature Communications*, vol. 15, no. 1, p. 8648, 2024, doi: 10.1038/s41467-024-52916-z.

[10] S. Barber, V. Gomez-Godinez, J. Young, A. Wei, S. Chen, A. Snissarenko, S. S. Chan, C. Wu, and L. Shi, "Impacts of H2O2, SARM1 inhibition, and high NAm concentrations on Huntington's disease laser-induced degeneration," *Journal of Biophotonics*, vol. 17, no. 3, p. e202300370, 2024, doi: 10.1002/jbio.202300370.

[11] Y. Gu, F. Guerra, M. Hu, A. Pope, K. Sung, W. Yang, S. Jetha, T. A. Shoff, T. Gunatilake, O. Dahlkamp, L. Z. Shi, F. Manganelli, M. Nolano, Y. Zhou, J. Ding, C. Bucci, and C. Wu, "Mitochondria dysfunction in Charcot Marie Tooth 2B Peripheral Sensory Neuropathy," *Communications Biology*, vol. 5, no. 1, p. 717, 2022, doi: 10.1038/s42003-022-03632-1.

[12] V. Gomez Godinez, V. Morar, C. Carmona, Y. Gu, K. Sung, L. Z. Shi, C. Wu, D. Preece, and M. W. Berns, "Laser-Induced Shockwave (LIS) to Study Neuronal Ca2+ Responses," *Frontiers in Bioengineering and Biotechnology*, vol. 9, p. 598896, 2021, doi: 10.3389/fbioe.2021.598896.

[13] J. Zhou, F. Tian, J. Hu, Z. L. Shi, V. G. Godinez, D. P. Tsai, and Z. Liu, "Eagle-Eye Inspired Meta-Device for Phase Imaging," *Advanced Materials*, vol. 36, no. 32, p. e2402751, 2024, doi: 10.1002/adma.202402751.

[14] Y. Pan, L. Z. Shi, C. W. Yoon, D. Preece, V. Gomez-Godinez, S. Lu, C. Carmona, S. H. Woo, S. Chien, M. W. Berns, L. Liu, and Y. Wang, "Mechanosensor Piezo1 mediates bimodal patterns of intracellular calcium and FAK signaling," *EMBO Journal*, vol. 41, no. 17, p. e111799, 2022, doi: 10.15252/embj.2022111799.

[15] Y. Gu, A. Pope, C. Smith, C. Carmona, A. Johnstone, L. Shi, X. Chen, S. Santos, C. C. Bacon-Brenes, T. Shoff, K. M. Kleczko, J. Frydman, L. M. Thompson, W. C. Mobley, and C. Wu, "BDNF and TRiC-inspired reagent rescue cortical synaptic deficits in a mouse model of Huntington's disease," *Neurobiology of Disease*, vol. 195, p. 106502, 2024, doi: 10.1016/j.nbd.2024.106502.

[16] A. B. Stilgoe, I. A. Favre-Bulle, M. L. Watson, V. Gomez-Godinez, M. W. Berns, D. Preece, and H. Rubinsztein-Dunlop, "Shining Light in Mechanobiology: Optical Tweezers, Scissors, and Beyond," *ACS Photonics*, vol. 11, no. 3, pp. 917–940, 2024, doi: 10.1021/acsphotonics.4c00064.

[17] H. Wang, S. Li, H. Zhang, Y. Wang, S. Hao, and X. Wu, "BLM prevents instability of structure-forming DNA sequences at common fragile sites," *PLoS Genetics*, vol. 14, no. 11, p. e1007816, 2018, doi: 10.1371/journal.pgen.1007816.

[18] X. Kong, S. K. Mohanty, J. Stephens, J. T. Heale, V. Gomez-Godinez, L. Z. Shi, J. Kim, K. Yokomori, M. W. Berns, "Comparative analysis of different laser systems to study cellular responses to DNA damage in mammalian cells", *Nucleic Acids Research*, Volume 37, Issue 9, 1 May 2009, Page e68, https://doi.org/10.1093/nar/gkp221

[19] Y. Lian, Y. Liu, D. Cheng, C. Chi, Y. Bao, Y. Wang. "Dual-mode varifocal Moiré metalens for quantitative phase and edge-enhanced imaging." Nanophotonics. 2025 Aug 6;14(18):3053-3062. doi:

10.1515/nanoph-2025-0245. PMID: 40970243; PMCID: PMC12442366.

[20] Y. Li, P. Chang, S. Sankaran, H. Jang, Y. Nie, A. Zeng, S. Hussain, J. Y. Wu, X. Chen, L. Shi. Bioorthogonal Stimulated Raman Scattering Imaging Uncovers Lipid Metabolic Dynamics in *Drosophila* Brain During Aging. GEN Biotechnol. 2023 Jun 1;2(3):247-261. doi: 10.1089/genbio.2023.0017. Epub 2023 Jun 19. PMID: 37363411; PMCID: PMC10286263.